Published OnlineFirst August 12, 2019; DOI: 10.1158/2326-6066.CIR-19-0103

Research Article

Cancer Immunology Research

Human CD4$^+$ T Cells Specific for Merkel Cell Polyomavirus Localize to Merkel Cell Carcinomas and Target a Required Oncogenic Domain

Natalie V. Longino[1,2], Junbao Yang[3], Jayasri G. Iyer[1], Dafina Ibrani[1], I-Ting Chow[3], Kerry J. Laing[4], Victoria L. Campbell[4], Kelly G. Paulson[1,5,6], Rima M. Kulikauskas[1], Candice D. Church[1], Eddie A. James[3], Paul Nghiem[1,2], William W. Kwok[3], and David M. Koelle[3,4,7,8,9]

Abstract

Although CD4$^+$ T cells likely play key roles in antitumor immune responses, most immuno-oncology studies have been limited to CD8$^+$ T-cell responses due to multiple technical barriers and a lack of shared antigens across patients. Merkel cell carcinoma (MCC) is an aggressive skin cancer caused by Merkel cell polyomavirus (MCPyV) oncoproteins in 80% of cases. Because MCPyV oncoproteins are shared across most patients with MCC, it is unusually feasible to identify, characterize, and potentially augment tumor-specific CD4$^+$ T cells. Here, we report the identification of CD4$^+$ T-cell responses against six MCPyV epitopes, one of which included a conserved, essential viral oncogenic domain that binds/disables the cellular retinoblastoma (Rb) tumor suppressor. We found that this epitope ($WED_{LT209\text{-}228}$) could be presented by three population-prevalent HLA class II alleles, making it a relevant target in 64% of virus-positive MCC patients. Cellular staining with a $WED_{LT209\text{-}228}$–HLA-DRB1*0401 tetramer indicated that specific CD4$^+$ T cells were detectable in 78% (14 of 18) of evaluable MCC patients, were 250-fold enriched within MCC tumors relative to peripheral blood, and had diverse T-cell receptor sequences. We also identified a modification of this domain that still allowed recognition by these CD4$^+$ T cells but disabled binding to the Rb tumor suppressor, a key step in the detoxification of a possible therapeutic vaccine. The use of these new tools for deeper study of MCPyV-specific CD4$^+$ T cells may provide broader insight into cancer-specific CD4$^+$ T-cell responses.

Introduction

Merkel cell carcinoma (MCC) is a rare but deadly skin cancer with a relative mortality rate of 46%, making it approximately three times as deadly as malignant melanoma on a per-case basis (1). The current annual U.S. incidence of ~2,500 cases per year is projected to climb to ~3,200 by the year 2025 (2). This predicted increase is due to the unusually strong association of age with MCC and the aging of the "Baby Boomer" generation (2). In the United States, the majority of MCCs (~80%) are etiologically linked to the Merkel cell polyomavirus (MCPyV; ref. 3), a small (~5.4 kilobase genome) double-stranded DNA virus that encodes oncogenic T-antigens, including large T (LT) and small T (sT; ref. 3). Importantly, elimination of the C-terminal region of LT (necessary for viral DNA replication) is an invariant requirement for oncogenesis. In contrast, MCCs retain the N-terminal region, which promotes cell-cycle progression and contains the "LxCxE motif" (4, 5). The LxCxE-binding motif is conserved in LT among human polyomaviruses and several other DNA viruses, suggesting that manipulation of retinoblastoma (Rb) biology is critical for viral pathogenesis (6). Interestingly, the LxCxE domain in several DNA viruses was recently shown to mediate direct binding to STING and, thus, antagonize the cyclic GMP-AMP synthase (cGAS) innate antiviral interferon pathway (7), which may further increase the selective pressure to maintain this sequence. Consequently, the MCPyV T-antigens, which are mechanistically involved in tumor formation, are both attractive targets for the study of tumor-specific T-cell responses and rational candidates for specific immunotherapy (8, 9).

The importance of immune cell function in MCC is highlighted by the fact that MCC patients exhibit high response rates to PD-1 blocking agents (10–12). Robust CD8$^+$ T-cell intratumoral infiltration is associated with 100% disease-specific survival, independent of stage at diagnosis (13, 14). However, this favorable

[1]Department of Medicine, Division of Dermatology, University of Washington, Seattle, Washington. [2]Department of Pathology, University of Washington, Seattle, Washington. [3]Translational Research Program, Benaroya Research Institute at Virginia Mason, Seattle, Washington. [4]Department of Medicine, Division of Allergy and Infectious Disease, University of Washington, Seattle, Washington. [5]Clinical Research Division, Fred Hutchinson Cancer Research Center, Seattle, Washington. [6]Department of Medicine, Division of Medical Oncology, University of Washington, Seattle, Washington. [7]Department of Laboratory Medicine, University of Washington, Seattle, Washington. [8]Department of Global Health, University of Washington, Seattle, Washington. [9]Vaccine and Infectious Diseases Division, Fred Hutchinson Cancer Research Center, Seattle, Washington.

Note: Supplementary data for this article are available at Cancer Immunology Research Online (http://cancerimmunolres.aacrjournals.org/).

P. Nghiem, W.W. Kwok, and D.M. Koelle contributed equally to this article.

Corresponding Author: Paul Nghiem, University of Washington, 850 Republican Street, Brotman Room 240, Seattle, WA 98109. Phone: 206-221-4594; Fax: 206-221-4364; E-mail: pnghiem@uw.edu

Cancer Immunol Res 2019;7:1727–39

doi: 10.1158/2326-6066.CIR-19-0103

Published OnlineFirst August 12, 2019; DOI: 10.1158/2326-6066.CIR-19-0103

pattern is only observed in 4% to 18% of patients (13, 14). In light of this link between local $CD8^+$ T cells and MCC survival, we sought to explore mechanisms that could regulate the $CD8^+$ T-cell response, including the adequacy of $CD4^+$ T-cell help. $CD4^+$ T cells are known to provide crucial support for $CD8^+$ T-cell function in a variety of settings. Cellular therapies utilizing $CD4^+$ chimeric antigen receptor (CAR) T-cell products (15), autologous $CD4^+$ T cells (16), or T-cell receptor (TCR)–transgenic $CD4^+$ T cells (17, 18) have mediated cancer regression. Therapeutic cancer vaccines primarily targeting $CD4^+$ T cells can induce epitope spreading of $CD8^+$ T-cell responses (19) and have shown promise in treating melanoma (20, 21). These findings suggest that $CD4^+$ T cells significantly contribute to cancer immune-based therapies. However, the low frequencies of antigen-specific $CD4^+$ T cells within peripheral blood (several logs lower than antigen-specific $CD8^+$ T cells) combined with a lack of specific tools to identify these cells have hindered their study. Consequently, we optimized and used a suite of complementary methods to identify MCPyV-specific $CD4^+$ T cells with the goal of enabling detailed tetramer-based characterization of $CD4^+$ T-cell responses against MCPyV and of contributing to the development of novel therapeutic strategies for MCC patients.

Materials and Methods

Subjects and specimens

Studies were approved by the Fred Hutchinson Cancer Research Center (FHCRC) and the Benaroya Research Institute (BRI) Institutional Review Boards and conducted according to the Declaration of Helsinki principles. Informed written consent was received from all participants. Subjects were HLA class II typed via polymerase chain reaction (PCR)–based methods at Bloodworks Northwest (Seattle, WA), by high-throughput next-generation sequencing at Scisco Genetics (FHCRC) as described (22) or by real-time PCR at BRI as described (23). We screened 89 MCC patients for appropriate HLA types from our repository of over 1,400 patients. Of those, 5 patients with available tumor material had HLA types we could study. Peripheral blood mononuclear cells (PBMC) were obtained from heparinized blood from MCC patients and healthy donors with Lymphocyte Separation Medium (Corning) and cryopreserved in freezing medium [50% human serum (Valley Biomedical), 40% RPMI (Thermo Fisher), and 10% DMSO (Thermo Fisher)]. Fresh MCC tumor material and punch biopsies (>1 cm^3) were processed into single-cell digests by mincing them into small pieces with sterile forceps and scissors, followed by incubation in 20 mL of digestion medium composed of RPMI plus 0.002 g DNase (Worthington Biochemical), 0.008 g collagenase (Worthington Biochemical), and 0.002 g hyaluronidase (Worthington Biochemical) in a 10-cm dish at 37°C with frequent, gentle swirling. After 3 hours of digestion, cells were strained through a 70-μm filter, centrifuged, resuspended in freezing medium (as described above), and cryopreserved. Tumor-infiltrating lymphocytes (TIL) were expanded for 2 weeks as described (24) before analysis. Briefly, minced tumor biopsies were cultured in T-cell medium [TCM; RPMI, 8% human serum, 200 nmol/L L-glutamine, and penicillin–streptomycin (100 U/mL; Thermo Fisher)] as described (25). Lymphoblastoid cell lines (LCL) were derived from PBMCs and maintained in LCL medium [RPMI, 10% fetal bovine serum, 200 nmol/L L-glutamine, penicillin–streptomycin (100 U/mL), 55 μmol/L 2-Mercaptoethanol (Thermo Fisher), and 1 mmol/L sodium pyruvate (Thermo Fisher)] as described (24).

Cell lines

MCC cell lines WaGa, MKL-1, and MCC-13 were cultured in RPMI-1640 supplemented with 10% fetal bovine serum (Atlantic Biologicals), 200 nmol/L L-glutamine, and penicillin–streptomycin (100 U/mL). WaGa cells were a gift from Dr. Juergen Becker, German Cancer Research Center, Heidelberg, Germany (8), MKL-1 cells from Masa Shuda (26), and MCC-13 cells from Helen Leonard (27). All cells, except COS-7, were confirmed authentic with short-tandem repeat analysis (STR; ATCC) and were *Mycoplasma* negative via PlasmoTest (InvivoGen). COS-7 cells (ATCC, CRL-1651, 2005) were maintained in DMEM supplemented with 10% FBS, 200 nmol/L L-glutamine, and penicillin–streptomycin (100 U/mL), and were free of *Mycoplasma*.

Tumor cell line reactivity determination

To examine the reactivity with intact tumor antigen, cell lysates of MCPyV-positive cell lines (WaGa and MKL-1) and of the MCPyV-negative MCC cell line (MCC-13) were used. The resulting supernatants were used as antigen (or control nonantigen) in the IFNγ intracellular cytokine staining assays described below.

Epitope determination

MCPyV oncoprotein $CD4^+$ T-cell epitopes were identified using three approaches: tetramer-guided epitope mapping (TGEM), intracellular cytokine staining (ICS), and carboxyfluorescein succinimidyl ester (CFSE) dilution.

For TGEM studies (28), PBMCs obtained from 24 healthy donors expressing at least one of eight discrete HLA class II allele types were cultured in TCM in the presence of pools of five MCPyV 20-mer peptides (GenScript; Supplementary Table S1) at 1 μg/mL final concentration of each peptide for 10 to 14 days. Subsequently, expanded PBMCs were subjected to two rounds of tetramer staining (first by tetramers loaded with a pool of five consecutive overlapping peptides and then with individual peptide-loaded tetramers corresponding to positive pools) as previously described (28). Tetramers were generated at the BRI for the following alleles: HLA-DRB1*0301, HLA-DRB1*0401, HLA-DRB1*0404, HLA-HLA-DRB1*0701, HLA-DRB1*1501, HLA-DRB5*0101, and HLA-DQB1*0602. Flow cytometry stains identified live $CD4^+$ (BioLegend, #344618) cells containing tetramer pool–positive cells and excluded $CD8^+$ (Invitrogen, MHCD0805), $CD14^+$ (BioLegend, #301828), and $CD19^+$ (BioLegend, #302232) cells. Cultures were then stained with single tetramers containing relevant peptides within the positive pool (Table 1). Four HLA alleles yielded MCPyV epitopes (HLA-DRB1*0301, HLA-DRB1*0401, HLA-DRB5*0101, and HLA-DQB1*0602), and for each allele type, four individuals were tested (Fig. 1). The fraction of patients with a given allele in which tetramer-positive cells were detected is denoted in Table 1.

For ICS assays focusing on IFNγ secretion, peptide pools composed of 17 to 27 peptides (13-mers) at final concentrations of 1 μg/mL of each peptide were incubated with 2.5×10^5 to 5×10^5 TILs and an equal number of autologous PBMCs as antigen-presenting cells (APC) for 16 hours as previously described (24). Data were acquired on a Canto RUO cytometer (Becton Dickinson). Flow cytometry analysis evaluated the percentage of

Published OnlineFirst August 12, 2019; DOI: 10.1158/2326-6066.CIR-19-0103

Table 1. Newly identified CD4 T-cell responses against MCPyV oncoprotein peptides

Name of peptide (first 3 AA)	Peptide sequence (core sequence underlined)	Location in MCPyV[a]	HLA restriction	Tet available?	T-cell source	Detected in: Healthy donors (expanded[b])	Detected in: Healthy donors (*ex vivo*)	MCC pts	Method(s) of identification
"MDL"	MDLVLNRKEREAL	CT-1-13	Undetermined	No[c]	PBMC	ND	ND	1/1	ICS
"GNI"	GNIPLMKAAFKRSCLKHHPD	CT-25-44	DRB5*0101	Yes	PBMC	1/4	ND	1/1	TGEM, ICS
"PVI"	PVIMMELNTLWSK	CT-49-61	Undetermined	No[c]	TIL	ND	ND	1/1	ICS
"NSG"	NSGRESSTPNGTSVPRNSSR	LT-185-204	DQB1*0602	Yes	PBMC	1/4	ND	1/1	TGEM, ICS
"PNG"	PNGTSVPRNSSRTYGTWEDL	LT-193-212	DQB1*0602	Yes	PBMC	1/4	ND	1/1	TGEM, ICS
"WED"	WEDLFCDESLSSP	LT-209-221	DQB1*0301	No[c]	TIL/PBMC	ND	ND	1/1	ICS
"WED"	WEDLFCDESLSSPEPPSSSE	LT-209-228	DRB1*0401	Yes	TIL/PBMC	4/4	8/10	14/18	TGEM, ICS
"WED"	WEDLFCDESLSSPEPPSSSE	LT-209-228	DRB1*0301	Yes	PBMC	3/4	ND	1/4	TGEM
"CIS"	CISCKLSRQHCSLKTLKQKN	sT-121-140	DRB1*0401	No[d]	PBMC	ND	ND	1/1	CFSE dilution, ICS

Abbreviation: ND, not done.

[a]The first 78 AA of LT and sT are shared and are referred to as "common T" or CT.

[b]Cells were expanded in the presence of 10 peptide pools (20-mers) for 10 to 14 days prior to staining.

[c]Tetramer synthesis not attempted due to lack of specific HLA restriction or unavailability of specific HLA allele type.

[d]Tetramer generation attempted but unsuccessful.

live IFNγ$^+$ (BD Pharmingen, 554701) CD4$^+$ cells and excluded dead (LIVE/DEAD Fixable Violet Dead Cell Stain, Invitrogen, #L34955), CD8$^+$, CD14$^+$, and CD19$^+$ cells.

For CFSE dilution (29), PBMCs from 3 MCC patients were stained with CFSE (Vybrant CFDA SE cell tracer kit, Invitrogen cat. #V-12883) following the manufacturer's instructions and incubated in RPMI-1640 containing 10% human serum, 2 mmol/L L-glutamine (HyClone), and 1% penicillin/streptomycin (HyClone) at a concentration of 4×10^6 cells per well in a 24-well plate. Two peptide pools composed of 24 peptides (20-mers overlapping by 12 AA; GenScript; Supplementary Table S1) were incubated with CFSE-labeled PBMCs at final concentrations of 1 μg/mL for each peptide for 5 days. Flow cytometry analysis evaluated the percentage of CFSE dilution among CD3$^+$ (ECD; Beckman Coulter; cat. #IM2705U) CD4$^+$ cells (PE; BioLegend; cat. #357404), excluding dead (7-AAD$^+$; BD Biosciences; cat. #559925).

In each of these methods, positive signals using peptide pools were confirmed through follow-up assays using individual peptides to define epitopes. The MCPyV CD4 epitopes discovered and validated through these complementary methods are summarized in Table 1.

For 1 patient in whom $WED_{LT209\text{-}228}$ specificity was based on IFNγ secretion (Fig. 2A), generated T-cell clones (described in the next section) were then tested for production of IFNγ following exposure to antigen in the presence of HLA class II locus–specific blocking mAbs (30) in order to determine HLA class II allele restriction (Fig. 2B). The IFNγ flow cytometry release assay was the same protocol as described above, with the exception that APCs were incubated for 10 minutes at room temperature with HLA blocking antibodies, L243 (HLA-DR), and SPVL3 (HLA-DQ) prior to the addition of responder cells with antigenic peptide. Antibodies pan-specific for blocking all HLA-DR (clone L243), HLA-DP (clone B7.21), or HLA-DQ (clone SPVL3) allelic variants were generated from murine hybridoma cell lines (31) and stored as crude supernatants at −80°C. Supernatants were used at a final 1:8 dilution for blocking.

T-cell sorting

$WED_{LT209\text{-}228}$–specific CD4$^+$ T cells were sorted using tetramer-based single-cell sorting, IFNγ capture, or CFSE dilution staining. Clones were derived from either expanded TIL cultures or peptide-stimulated PBMCs expanded as previously described (24, 28).

For tetramer-based sorting, PBMCs or TILs (5×10^6–20×10^6) were thawed, phosphate-buffered saline (PBS) washed, and incubated with 100 nmol/L dasatinib (SelleckChem, #S1021) for 10 minutes at 37°C in TCM (RPMI, 8% human

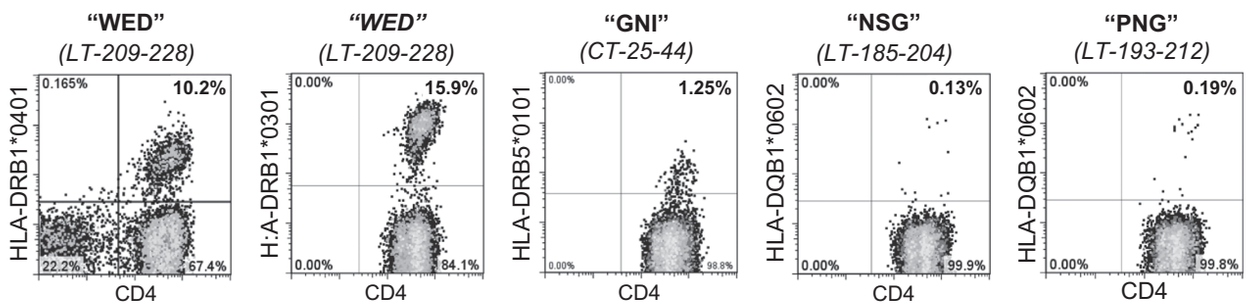

Figure 1.

TGEM identified four peptides presented by four population-prevalent HLA class II alleles. TGEM was performed as outlined in the Materials and Methods testing seven allele types. PBMCs were cultured in the presence of pools of five MCPyV 20-mer peptides (WED, GNI, NSG, PNG; AA sequence indicated) for 10 to 14 days, followed by staining for pools of tetrameric complexes of 10 peptides (composed of two combined pools) bound to HLA class II molecules. After identification of CD4$^+$tetramer$^+$ T cells, the same cultures were stained with single tetramers containing each relevant peptide within the positive pool. Representative flow plots are shown for each peptide. For each epitope, 4 individuals were tested, and 1 to 4 persons were positive, as detailed in column 7 of Table 1. The percentage of viable CD4$^+$tetramer$^+$ T cells (negative for CD8/CD14/CD19) in the lymphocyte forward/side scatter region is denoted.

Published OnlineFirst August 12, 2019; DOI: 10.1158/2326-6066.CIR-19-0103

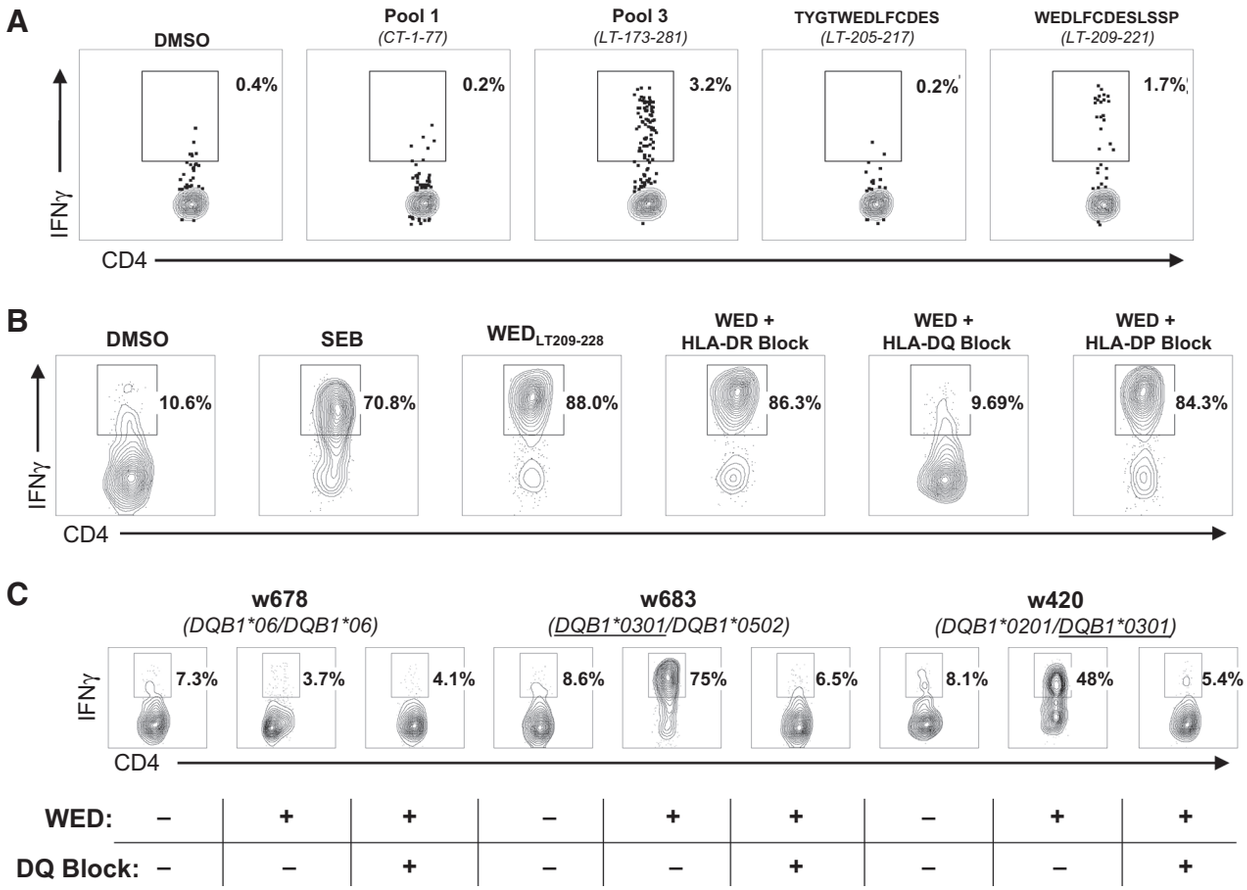

Figure 2.

The $WED_{LT209-228}$ epitope is presented by HLA-DRB1*0401, HLA-DRB1*0301, and HLA-DQB1*0301 alleles. **A,** ICS screening of expanded TILs from an MCC patient biopsy incubated with four MCPyV T-antigen 13-mer peptide pools (two shown). Reactive pool 3 was broken down into individual 13-mer peptides (two shown). The percentage of viable $CD4^+IFN\gamma^+$ T cells (CFSE-labeled APCs excluded and negative for CD8/CD14/CD19) in the lymphocyte forward/side scatter region is denoted. Negative control: TILs stimulated with DMSO and the peptide "TYGWEDLFCDES," which is 4 AA N-terminal to the "WED" peptide. Positive control: TILs stimulated with SEB. **B,** A $WED_{LT209-228}$–specific clone ± anti-HLA class II locus–specific blocking mAbs established HLA-DQ as the restricting locus. The percentage of viable $CD4^+IFN\gamma^+$ T cells (CFSE-labeled APCs excluded and negative for CD8/CD14/CD19) in the lymphocyte forward/side scatter region is denoted. Negative control: DMSO stimulated; positive control: SEB stimulated. **C,** HLA-DQB1*0301 restriction was established using LCLs from 3 different patients ("w678," "w683," and "w420") with defined HLA-DQ genotype with a $WED_{LT209-228}$–specific $CD4^+$ T-cell clone, peptide ("WED"), and inclusion of anti–HLA-DQ mAb ("DQ-Block"). The percentage of viable $CD4^+IFN\gamma^+$ T cells (negative for CD8/CD14/CD19) in the lymphocyte forward/side scatter region is denoted. DMSO and SEB were used as negative and positive controls, respectively. Plots shown represent one of two replicates.

serum, 200 nmol/L L-glutamine, and 100 U/mL penicillin–streptomycin). Cells were washed and resuspended in 50 μL TCM, stained with 2 μL of DRB1*0401-$WED_{LT209-228}$-PE tetramer (BRI), and incubated for 1 hour in the dark at room temperature. Cells were washed with 3 mL of 4°C, 1% BSA in PBS (PBS-A), collected by centrifugation, and resuspended in 500 μL PBS-A and enriched immunomagnetically for PE-positive cells following the manufacturer's instructions (STEMCELL Technologies, #18551). Enriched cells were washed in 2 mL 4°C PBS-A, resuspended in 50 μL of 1:2,000 diluted LIVE/DEAD Fixable Violet Dead Cell Stain (Invitrogen, #L34955), and incubated at 25°C for 20 minutes. Cells were then washed in 2 mL of 4°C PBS-A, resuspended in 95 μL of Fc block (STEMCELL Technologies, #18551) and stained with anti-CD4–Alexafluor 488 (BioLegend, #344618), anti-CD8–APC (Invitrogen, MHCD0805), anti-CD14–PacBlue (BioLegend, #301828), and anti-CD19–PacBlue (BioLegend, #302232). Following a 25-minute incubation on ice, cells were washed 2× with ice-cold PBS-A and resuspended in 150 μL of 2% human serum in RPMI. Viable $CD4^+$tetramer$^+$ cells (negative for CD8/CD14/CD19) in the lymphocyte forward/side scatter region were sorted into 96-well plates containing 100 μL TCM. For single-cell sorting using IFNγ capture, the IFNγ secretion enrichment kit (Miltenyi Biotec, #130-054-201) was used as per the manufacturer's instructions. T cells were sorted on an Aria II cell sorter (Becton Dickinson), and data were collected using Becton Dickinson FACSDiva software (v6.1.1). For sorting using CFSE dilution, cells were stained and stimulated with peptide as described above.

T-cell expansion

Cells sorted using one of the three methods described above were expanded for 2 weeks in 96-well plates with allogeneic irradiated feeder PBMCs (150,000 cells/well) and

Published OnlineFirst August 12, 2019; DOI: 10.1158/2326-6066.CIR-19-0103

phytohemagglutinin (PHA; 1.6 μg/mL) as described (32). After 24 hours, rIL15 (20 ng/mL; R&D Systems, #247-ILB-025) and natural IL2 (32 U/mL; Hemagen Diagnostics, #906011) were added. After 2 weeks, microcultures with visible growth were screened for specificity via ELISA or tetramer staining (described subsequently). Confirmed peptide-specific clones were further expanded in the presence of irradiated feeder cells, rIL2 (50 IU/mL; R&D Systems, #202-IL-010), and OKT3 (30 ng/mL; Miltenyi Biotec, #130-093-387) as described (24) plus rIL15 (20 ng/mL). Clones generated for these experiments are listed in Supplementary Table S2.

IFNγ and proliferation T-cell activation assays

The responsiveness of MCC patient WED$_{LT209\text{-}228}$–specific CD4$^+$ T-cell clones was evaluated as previously described (24). Briefly, T-cell clones from 5 individuals (listed in Supplementary Table S2) were stimulated with antigen (1 μg/mL of the WED$_{LT209\text{-}228}$ 20-mer peptide or 1:100 dilution of tumor cell line lysates) using autologous PBMCs from the same 5 individuals as APCs that were CFSE labeled to allow their exclusion from analysis (24). Cultures stimulated with dimethyl sulfoxide (DMSO) or staphylococcal enterotoxin B (SEB; 1 μg/mL; Thermo Fisher, NC0333616) were included as a negative and a positive control, respectively. Cells were stained for intracellular IFNγ and analyzed with FlowJo (version 10.4.0, FlowJo LLC), and viable IFNγ$^+$CD4$^+$ cells (negative for CD8/CD14/CD19) in the lymphocyte forward/side scatter region were designated as responder cells from the lymphocyte population. Some functional assays used cloned CD4$^+$ T-cell responders and ^{3}H-thymidine–based proliferation measurement as previously described (31).

Minimal epitope determination

To determine the minimal antigenic motif for positive 20-mers, 11-mer peptides overlapping by 10 AA were synthesized spanning the entire 20-mer (listed in Fig. 3; GenScript). ICS was performed as described previously (24). Briefly, autologous PBMCs were CFSE labeled to allow dump-gating, and cocultured with responder T cells and peptide as described above. Flow cytometric analysis was done on viable IFNγ$^+$CD4$^+$ cells (negative for CD8/CD14/CD19) in the lymphocyte forward/side scatter region. These cells were designated as responder cells in ICS assays.

IFNγ ELISA assays

WED$_{LT209\text{-}228}$–specific T-cell functional avidity was determined by coincubating HLA-DRB1*0401–restricted WED$_{LT209\text{-}228}$ T-cell clones and autologous PBMCs (1:1 ratio, 2×10^5 cells/well each) in 200 μL TCM with 10-fold serial-diluted antigenic peptides at final concentrations of 10^{-6} to 10^{-14} g/mL for 16 hours. Cross-reactivity against homologous regions of 12 additional human polyomaviruses was assessed by incubating HLA-DRB1*0401–restricted WED$_{LT209\text{-}228}$ T-cell clones and autologous PBMCs (1:1 ratio, 2×10^5 cells/well each) in 200 μL TCM with 13-mer peptides (Supplementary Table S3) at a final concentration of 1 μg/mL for 16 hours. To determine the reactivity of HLA-DRB1*0401–restricted WED$_{LT209\text{-}228}$ T-cell clones against wild-type versus S220-phosphorylated WED$_{LT209\text{-}228}$, HLA-DRB1*0401–restricted WED$_{LT209\text{-}228}$ T-cell clones were incubated with autologous PBMCs (1:1 ratio, 2×10^5 cells/well each) in 200 μL TCM with 20-mer wild-type WED$_{LT209\text{-}228}$ or S220-phosphorylated WED$_{LT209\text{-}228}$ (GenScript) peptides at a final concentration of 1 μg/mL for 16 hours. Concentrations of secreted IFNγ in cell culture supernatants were determined by ELISA (Affymetrix, #88-7316-76). To calculate EC$_{50,}$ IFNγ concentrations versus peptide concentrations were analyzed via nonlinear regression using Prism version 7.0 (GraphPad Software, Inc.).

LT antigen production and site-directed mutagenesis

The expression plasmid for the LT antigen fusion protein (pDEST103-GFP-LT) was created using Gateway recombination cloning technology (Thermo Fisher Scientific) to insert LT from pCMV-MCV156 into pDEST103 (33). The resulting plasmid expresses the eGFP-LT fusion protein under the control of the CMV promoter. Site-directed mutagenesis (New England Biolabs, #E0554S) was performed to generate LT S220A and LT E216K

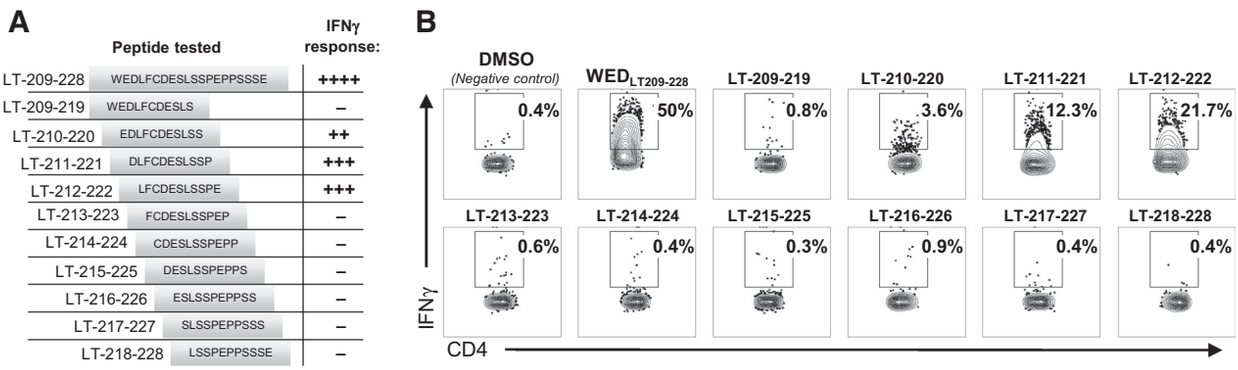

Figure 3.

The "WED" minimal epitope presented by HLA-DRB1*0401 encompasses the Rb-binding motif. **A,** Schematic of peptides synthesized for testing minimal epitope. **B,** A "WED"-specific CD4$^+$ T-cell clone (wb688 clone 1,3) generated from a healthy donor, following *ex vivo* peptide-stimulated PBMC expansion, was incubated with a HLA-DRB1*0401 LCLs and stimulated with DMSO vehicle control, "WED" 20-mer (positive control), or internal 11-mer peptides overlapping by 10 AA within the "WED" 20-mer. The absence of responses to some 11-mer peptides provides an additional, internal negative control. Peptides were tested at 1 μg/mL and IFNγ responses measured by ICS assay. The percentage of viable CD4$^+$IFNγ$^+$ T cells (CFSE-labeled APCs excluded and negative for CD8/CD14/CD19) in the lymphocyte forward/side scatter region is denoted. These data are representative of DRB1*0401-restricted WED$_{LT209\text{-}228}$ –specific CD4$^+$ T-cell clones generated from 3 individuals as detailed using a secreted IFNγ readout in Supplementary Fig. S5A.

Published OnlineFirst August 12, 2019; DOI: 10.1158/2326-6066.CIR-19-0103

mutants with the following primer sets: forward primer 5′-GCGATGAATCACTTTCCGCTCCTGAGCCTC-3′ and reverse primer 5′-AGAAGAGATCCTCCCAGGTGCC-3′ for S220A; and forward primer 5′-CGACAAGTCACTTCCTCCCCTGAG-3′ and reverse primer 5′-CAGAACAGATCCTCCCAGGTGCCATC-3′ for E216K. Mutations at the specific sites were confirmed by sequencing. Protein was expressed by COS-7 cells (ATCC, CRL-1651, 2005). COS-7 cells were plated the day before transfection at 75,000 cells/well in 12-well plates in 0.5 mL of DMEM + 10% FBS, 200 nmol/L L-glutamine, and penicillin–streptomycin (100 U/mL), and pDEST103-GFP-LT was transfected into COS-7 cells using FuGENE HD (Promega, #E2311) as per the manufacturer's instructions. Seventy-two hours after transfection, eGFP-positive cells were sorted, and lysates were generated as described above. Clarified supernatants were used as the antigen in ICS assays as described above.

T-cell receptor beta sequencing and analysis of dextramer-sorted $WED_{LT209-228}$-specific cells

At least 3 million cells derived from fresh tumor digest of three HLA-DRB1*0401–positive MCC patients were stained with HLA-DRB1*0401-$WED_{LT209-228}$-PE dextramer (Immudex), and the same mAb cocktail as described for tetramer sorting plus LIVE/DEAD Fixable Violet (Invitrogen, #L34955). Viable dextramer$^+$CD4$^+$ cells (negative for CD14, CD19, and CD8) were bulk sorted using an Aria II cell sorter, flash frozen, and submitted to Adaptive Biotechnologies for genomic DNA extraction. Next-generation survey-level sequencing was used to determine T-cell receptor beta locus (*TRB*) CDR3 sequences with read normalization performed as described (33). All *TRB* CDR3 sequences detected at least twice were categorized as dextramer-positive clonotypes. Shannon entropy was calculated on the estimated number of genomes found twice or more for all productive *TRB* CDR3 reads and normalized by dividing the $\log_2$ of the number of unique productive sequences in each sample. Clonality was calculated as 1 minus normalized entropy. Sequences are available through Adaptive immuneACCESS (https://clients.adaptivebiotech.com/pub/longino-2019-cir).

Statistical analysis

Analyses were completed using Prism software, version 7, with a statistical significance threshold of 0.05. Specific tests used for each analysis are denoted in figure legends. Flow cytometry data were repeated with biological replicates, typically from the same subject and the same source of PBMCs or tumor specimens. Biological replicates were assessed on different assay dates. Therefore, statistical analyses across these experiments were not deemed appropriate.

Results

Identification of six CD4 epitopes within the MCPyV T-antigen oncoproteins

Our previously reported screens of expanded TILs and overlapping 13-mer peptides spanning the MCPyV T-antigens identified MCPyV-specific CD4$^+$ T cells responsive to TLWSKFQQNIHKL, located within the common T region (AA 57–69; $TLW_{CT57-69}$) shared by LT and sT (24). Using this same method, we subsequently identified two additional CD4 epitopes, WEDLFCDESLSSP ($WED_{LT209-221}$; Fig. 2A) and PVIMMELNTLWSK ($PVI_{CT49-61}$; Supplementary Fig. S1A). Histologic examination has previously revealed CD4$^+$ T-cell infiltration into or surrounding many MCPyV-positive MCC tumors (34); therefore, we suspected that many additional CD4 MCPyV epitopes were present but remained undetected via this initial approach. Consequently, we pursued complementary strategies for epitope discovery. We synthesized 20-mer peptides overlapping by 12 AA spanning MCPyV LT and sT (Supplementary Table S1) and used TGEM (28), IFNγ staining (24, 35), and CFSE dilution (29) following MCPyV peptide stimulation of PBMCs. Using these approaches, we identified four additional epitopes and verified reactivity to $WED_{LT209-228}$ in additional patients (Table 1; Supplementary Figs. S1B and S2–S14).

T cells that recognized $WED_{LT209-228}$ were detected by TGEM using both HLA-DRB1*0401 and HLA-DRB1*0301 tetramers (Fig. 1), indicating that the same epitope could be presented in the context of these two HLA class II alleles. To enhance detection of antigen-specific T cells, we generated an HLA-DRB1*0401-$WED_{LT209-228}$ dextramer, as dextramers are reported to have improved sensitivity compared with tetramers (36). Screening of peripheral blood samples using this dextramer indicated that $WED_{LT209-228}$ –specific CD4$^+$ T cells could be visualized directly *ex vivo* in the majority of HLA-DRB1*0401 patients (14 of 18, 77.8%) and healthy donors (8 of 10, 80%; Table 1).

The initial discovery of $WED_{LT209-228}$ using TILs from an HLA-DRB1*0401– and HLA-DRB1*0301–negative patient indicated that this peptide could also be presented by a non–HLA-DRB1*0401/DRB1*0301 allele (Fig. 2A). To determine this additional allele, PBMCs from the TIL donor in which $WED_{LT209-228}$ was initially identified were expanded in the presence of $WED_{LT209-228}$ peptide and sorted using IFNγ capture to generate clones (37). After confirming $WED_{LT209-228}$ specificity, T-cell clones were tested for production of IFNγ following exposure to antigen in the presence of HLA class II locus–specific blocking mAbs (ref. 30; Fig. 2B). Only anti–HLA-DQ blocked responses, indicating HLA-DQ restriction. The subject in which the $WED_{LT209-228}$ response was initially identified is heterozygous for HLA-DQB1*0301 and HLA-DQB1*0501. LCLs from HLA-genotyped donors (Fig. 2C) partially matched to the restricting DQB1 alleles were used as APCs. Only APCs bearing HLA-DQB1*0301 induced IFNγ responses from T-cell clones, and responses were blocked by anti–HLA-DQ. These data collectively indicated that $WED_{LT209-228}$ could be presented by DRB1*0401, DRB1*0301, and DQB1*0301. Among the MCC patients in our cohort for which we have class II HLA typing data (DRB1 locus, $n = 131$; DQB1 locus, $n = 53$), 64% expressed at least one of these three alleles. Consequently, this epitope is immunologically relevant for the majority of patients with MCPyV-positive tumors.

The epitope within $WED_{LT209-228}$ encompasses the LxCxE motif

CD4$^+$ T-cell epitopes typically range from 9 to 22 AA in length (38). We sought to determine the core sequence necessary for T-cell recognition within $WED_{LT209-228}$ in the context of HLA-DRB1*0401, the most prevalent allele of the three restriction elements in the general population that accommodated this epitope. HLA-DRB1*0401–expressing APCs were loaded with 11-mer peptides overlapping by 10 AA spanning $WED_{LT209-228}$ and incubated with $WED_{LT209-228}$–specific, HLA-DRB1*0401–restricted CD4 clones from 3 individuals (Supplementary Table S2) to identify its minimal epitope (Fig. 3). $WED_{LT209-228}$–specific clones responded to each 11-mer spanning LT-210-222, which share the 9 AA core LFCDESLSS (LT-212-220; Fig. 3).

Published OnlineFirst August 12, 2019; DOI: 10.1158/2326-6066.CIR-19-0103

Stimulation with this 9-mer did not elicit a significant response in three DRB1*0401-restricted $WED_{LT209-228}$–specific clones from the 3 individuals (Supplementary Fig. S5A), suggesting that flanking residues may stabilize and improve the strength of TCR stimulation and/or HLA binding as has been described (39). Importantly, this epitope encompasses the conserved LxCxE-binding motif that is critical for MCPyV LT binding to Rb. The minimal epitope presented by DQB1*0301 was found to be LT-210-219 (Supplementary Fig. S5B), whereas the minimal epitope presented by DRB1*0301 was not determined. Because the LxCxE motif is conserved among many DNA viruses, including the other described human polyomaviruses, four HLA-DRB1*0401–restricted $WED_{LT209-228}$ T-cell clones were incubated overnight with 13-mer peptides spanning the LxCxE motif of 12 additional human polyomaviruses with homologous regions (Supplementary Table S3). IFNγ secretion from $CD4^+$ T cells clones was detected against the MCPyV peptide (LT-210-222), as well as the homologous sequence from the human polyomavirus 9 (HuPyV9) for one clone and human polyomavirus 12 (HuPyV12) for three of the four clones (Supplementary Fig. S5C). These data indicated that the T-cell receptors expressed by these three clones could tolerate different degrees of variance and that cross-reactivity against other polyomaviruses was possible.

$CD4^+$ T cells recognize the $WED_{LT209-228}$ epitope in the context of MCC tumors

Phosphorylation of serine residue 220 adjacent to the MCPyV LT LxCxE motif is required for binding to Rb (ref. 40; Fig. 4A). To test whether $WED_{LT209-228}$–specific T cells tolerated this posttranslational modification, five HLA-DRB1*0401–restricted T-cell clones were assayed for recognition of wild-type (WED-WT) or phosphorylated-S220 (S220p) 20-mers (Fig. 4B). Functional avidity, expressed as EC_{50}, was calculated for the five DRB1*0401-restricted clones from 4 donors (2 MCC patients and 2 healthy controls; Fig. 4C). Functional avidities ranged over two orders of magnitude for WED-WT and one order of magnitude for S220p. Phosphorylation of S220 did not significantly change the EC_{50} for $WED_{LT209-228}$–specific $CD4^+$ T-cell clones collectively. However, the two clones derived from healthy donors did show a decrease in functional avidity against WED-S220p relative to WED-WT. Evaluation of a much larger number of clones from additional subjects would be necessary to determine whether this trend is significant. To evaluate whether the $WED_{LT209-228}$ epitope can be processed from the LT protein in MCC tumor cells, APCs (autologous PBMCs) and DRB1*0401-restricted $WED_{LT209-228}$–specific $CD4^+$ T clones (data from MCC patient z1107 clone 1 depicted, representing replicate data from 3 tested individuals) were incubated with lysates from two MCPyV-positive MCC cell lines, MKL-1 and WaGa, and an MCPyV-negative cell line, MCC-13. $WED_{LT209-228}$–specific $CD4^+$ T-cell clones responded specifically to the MCPyV-positive lysates (Fig. 4D). These data indicated that the LT protein was present in an immunogenic context in virus-positive MCC cell lines and suggest that $WED_{LT209-228}$ is naturally processed in the virus-positive MCC tumor context *in vivo*.

Virus-specific CD4 T cells are enriched within tumors and have diverse TCR repertoires

To determine if $WED_{LT209-228}$–specific cells infiltrate MCC tumors, we stained tumor digests from 3 MCC patients with the HLA-DRB1*0401-$WED_{LT209-228}$ dextramer. The percentage of $WED_{LT209-228}$–specific cells within the total tumor-infiltrating $CD4^+$ T cells ranged from 0.03% to 0.72% (median 0.56%; Fig. 5A). In contrast, PBMCs from 13 MCC patients were stained with the HLA-DRB1*0401-$WED_{LT209-228}$ dextramer, and the median frequency of $WED_{LT209-228}$–specific $CD4^+$ T cells within the periphery was significantly lower at 0.0022% of total $CD4^+$ T cells (Fig. 5B). These frequencies closely aligned with prior reports of peripheral virus-specific $CD4^+$ T-cell frequencies (41). These results indicated an enrichment of $WED_{LT209-228}$–specific $CD4^+$ T cells within MCC tumors compared with the periphery, suggesting active recruitment of these cells into the tumor microenvironment.

Next, we evaluated the clonal diversity of $WED_{LT209-228}$–specific $CD4^+$ T cells within MCC tumors by next-generation sequencing of the *TRB* from dextramer-sorted cells isolated from these tumor digests as previously described (33). Analysis of the *TRB* complementary determining region 3 (CDR3) sequences yielded 366 unique *TRB* AA sequences from the three tumors (Fig. 5C). Of the 366, two sequences were shared between patients "w876" and "w1056" (exploded, starred pie slices; Fig. 5C). These were identical at the AA but not nucleotide level, suggesting convergence. In order to estimate immunodominance within each tumor's $WED_{LT209-228}$–specific $CD4^+$ T-cell population, clonality scores were calculated (see Materials and Methods). The clonality score of the dextramer-sorted samples ranged from 0.111 to 0.137, indicating that although the *TRB* repertoires of infiltrating T cells within these MCC tumors were diverse, a few dominant clonotypes were expanded, with the top clonotype occupying 6.3% to 12.5% of the populations (Fig. 5C).

The S220A mutation within $WED_{LT209-228}$ retains immunogenicity

The data presented thus far suggest that the $WED_{LT209-228}$ epitope could be a therapeutically useful target, either for adoptive cellular therapy or in the context of a therapeutic cancer vaccine. However, inclusion of the LxCxE motif in a vaccine is not straightforward due to the Rb-binding, oncogenic activity of this domain. This issue has been addressed in human papillomavirus (HPV) vaccines by mutating the LxCxE motif to render the HPV-E7 oncoprotein nononcogenic (42). Two mutations within the LxCxE domain of MCPyV LT have been reported to inhibit oncogenic activity *in vitro*, E216K (4) and S220A (40). To test whether immunogenicity of the $WED_{LT209-228}$ epitope could be retained with either of these mutations, we created an antigen by transfecting COS-7 cells with wild-type LT (LT-WT), or the LT-S220A or LT-E216K mutants (33). As an experimental control, we also tested a mutant that has all three critical LxCxE residues mutated (LT-VxSxD). Lysates from LT-expressing cells were tested as antigen with autologous PBMCs as APCs and a $WED_{LT209-228}$–specific, HLA-DRB1*0401–restricted $CD4^+$ T-cell clone (wb688 clone 1,3). $WED_{LT209-228}$–specific clones responded to wild-type and MCPyV LT-S220A (Fig. 6A) but not to the "detoxified" E216K and VxSxD variants. To further compare the strength of response against LT-WT and LT-S220A, HLA-DRB1*0401–restricted $CD4^+$ T-cell clones were stimulated with serial dilutions of WED-WT and WED-S220A peptides (20-mers). The S220A variant stimulated clones derived from MCC patients more potently than WED-WT, as measured by EC_{50} for each

Published OnlineFirst August 12, 2019; DOI: 10.1158/2326-6066.CIR-19-0103

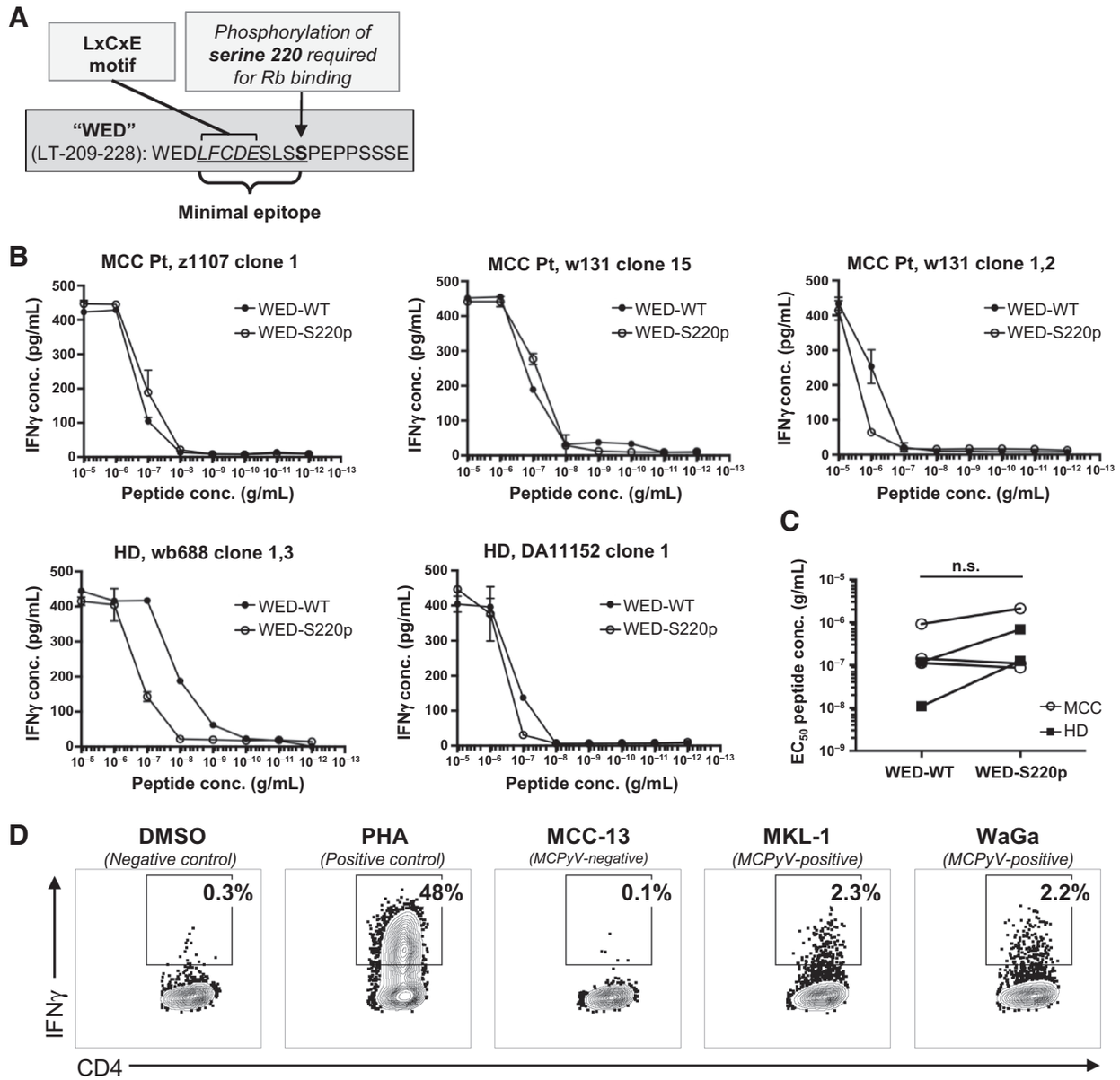

Figure 4.

HLA-DRB1*0401 $WED_{LT209-228}$–specific $CD4^+$ T-cell clones can recognize LT presented in the context of MCC tumors. **A,** Schematic of "WED" peptide features. **B,** Dose–response curves depicted for five $WED_{LT209-228}$–specific clones stimulated with $WED_{LT209-228}$ (WED-WT) or $WED_{LT209-228}$-S220p peptides. IFNγ secretion was measured by ELISA, and samples were run in duplicate. Lines connect means. Error bars denote standard deviation. Of the five clones tested, three were derived from MCC patients (MCC) and two were derived from healthy donors (HD). **C,** Dose–response curves were used to calculate the EC_{50} of five distinct "WED"-specific $CD4^+$ T-cell clones stimulated with either $WED_{LT209-228}$ or $WED_{LT209-228}$-S220p peptides. Clones from healthy donors are filled squares, and clones generated from MCC patients are open circles. Wilcoxon matched-pairs signed rank test was used to compare EC_{50} from clones stimulated with WED-WT or WED-S220p. n.s., not significant. **D,** $WED_{LT209-228}$ –specific clones were incubated with DRB1*0401-positive APCs and lysate from either MCPyV-negative (MCC-13) or MCPyV-positive (MKL-1 and WaGa) cell lines, DMSO (negative control), or PHA (positive control). The percentage of viable $CD4^+IFN\gamma^+$ T cells (CFSE-labeled APCs excluded and negative for CD8/CD14/CD19) in the lymphocyte forward/side scatter region is denoted. Flow plots are representative data of four distinct *TRB* CDR3 clonotypes.

responder CD4 clone, whereas little change was observed in the measured EC_{50} of clones derived from healthy donors (Fig. 6B). It will be important to test additional donors and MCC patients to validate whether this difference in response is consistently found between these two donor sources. However, these data do suggest that the LT-S220A mutant (reported not to bind Rb) retained and may even strengthen immune recognition of this region in the context of HLA-DRB1*0401. These data suggest that this mutation may be clinically useful in the design of a therapeutic cancer vaccine.

Published OnlineFirst August 12, 2019; DOI: 10.1158/2326-6066.CIR-19-0103

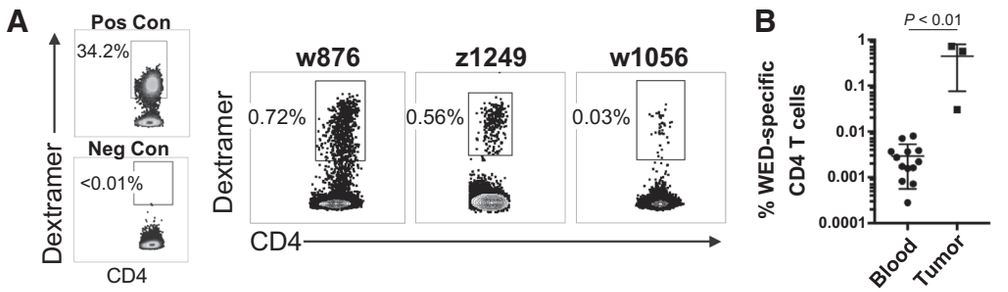

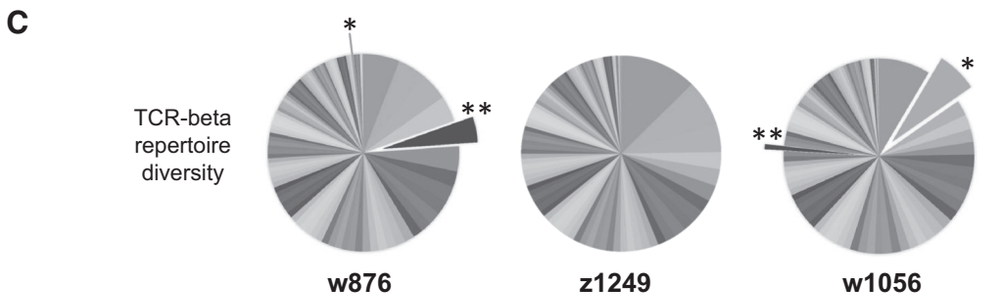

	w876	z1249	w1056
No. of cells sorted	529	380	195
No. of unique clonotypes	118	126	122
No. of shared clonotypes	2	0	2
Clonality of sample	0.111	0.16	0.137
Frequency of predominant clonotype	6.3%	12.5%	8.2%

Figure 5.

$WED_{LT209-228}$–specific $CD4^+$ T cells are enriched in MCC tumors and are diverse. **A,** Fresh tumor digest samples were acquired from 3 HLA-DRB1*0401–positive patients and stained with DRB1*0401-$WED_{LT209-228}$ dextramer. A $WED_{LT209-228}$ –specific CD4 clone generated against the $WED_{LT209-228}$ epitope was spiked into PBMCs as a positive control. TILs from an MCPyV-positive, HLA-DRB1*0401–negative patient were used as a negative control. Frequency of $CD4^+$dextramer$^+$ T cells is shown for the indicated clones. Positive dextramer staining was consistent between two replicate experiments. **B,** Peripheral blood samples ($n = 13$) and fresh tumor digest samples ($n = 3$) from HLA-DRB1*0401–positive MCC patients were stained with DRB1*0401-$WED_{LT209-228}$ dextramer as described in Materials and Methods. The percentage of viable $CD4^+$dextramer$^+$ T cells (negative for CD8/CD14/CD19) in the lymphocyte forward/side scatter region was divided by the total $CD4^+$ T-cell population (in the lymphocyte forward/side scatter region, viable $CD4^+CD8^-CD14^-CD19^-$). The median number of $WED_{LT209-228}$–specific $CD4^+$ T cells of the total CD4 population was 0.0022% in the periphery compared with 0.56% within tumors ($P = 0.0036$, Mann–Whitney test). **C,** TCR beta chain sequencing of the variable CDR3 region was performed on sorted cells from **A**. Pie slices depict the frequency of an individual clonotype within the dextramer-positive, $WED_{LT209-228}$–specific $CD4^+$ T-cell population. Exploded and starred slices indicate two *TRB* sequences with shared AA sequences between patients w876 and w1056.

Discussion

Here, we report six MCPyV $CD4^+$ T-cell epitopes, including a conserved and immunogenic $WED_{LT209-228}$ epitope within a key oncogenic region of the MCPyV LT antigen. The $WED_{LT209-228}$ epitope was recognized in the context of at least three discrete, population-prevalent HLA allelic variants. Within our HLA-typed MCC cohort, 64% expressed one or more of these alleles, indicating that this epitope was immunologically relevant in most MCC patients with MCPyV-positive tumors. Further supporting this notion, the $WED_{LT209-228}$ epitope encompasses the LxCxE motif, which is a critical binding site of the tumor suppressor Rb (4, 40). Persistent expression of this region is required for MCC tumor development and growth (4), and this sequence is conserved in MCC tumors. Indeed, of 99 MCPyV tumor–associated LT sequences in GenBank, only one has a coding variation within LT-212-220 (S219F; GenBank KJ128376.1). $WED_{LT209-228}$–specific T cells infiltrated each of three tested MCC tumors from DRB1*0401-positive patients, and $WED_{LT209-228}$–specific T cells were 250-fold enriched within these tumor samples compared with blood, as assessed by MHC-peptide multimer staining. These $WED_{LT209-228}$–specific T cells exhibited diverse TCR repertoires that include expanded clonotypes, suggesting *in vivo* antigen recognition and, consequently, that these T cells could home appropriately into tumor tissue and have therapeutic potential.

To date, tumor immunology research has largely focused upon studying and improving $CD8^+$ (rather than $CD4^+$) T-cell responses. This is due to the lower relative frequencies of antigen-specific $CD4^+$ T cells compared with $CD8^+$ T cells (~100–1000-fold; refs. 41, 43), making detailed characterization of tumor-specific $CD4^+$ T cells more difficult. The generation of HLA class II tetramers for the isolation and study of antigen-specific $CD4^+$ T cells poses numerous technical challenges (44). However, a growing body of evidence suggests that

Published OnlineFirst August 12, 2019; DOI: 10.1158/2326-6066.CIR-19-0103

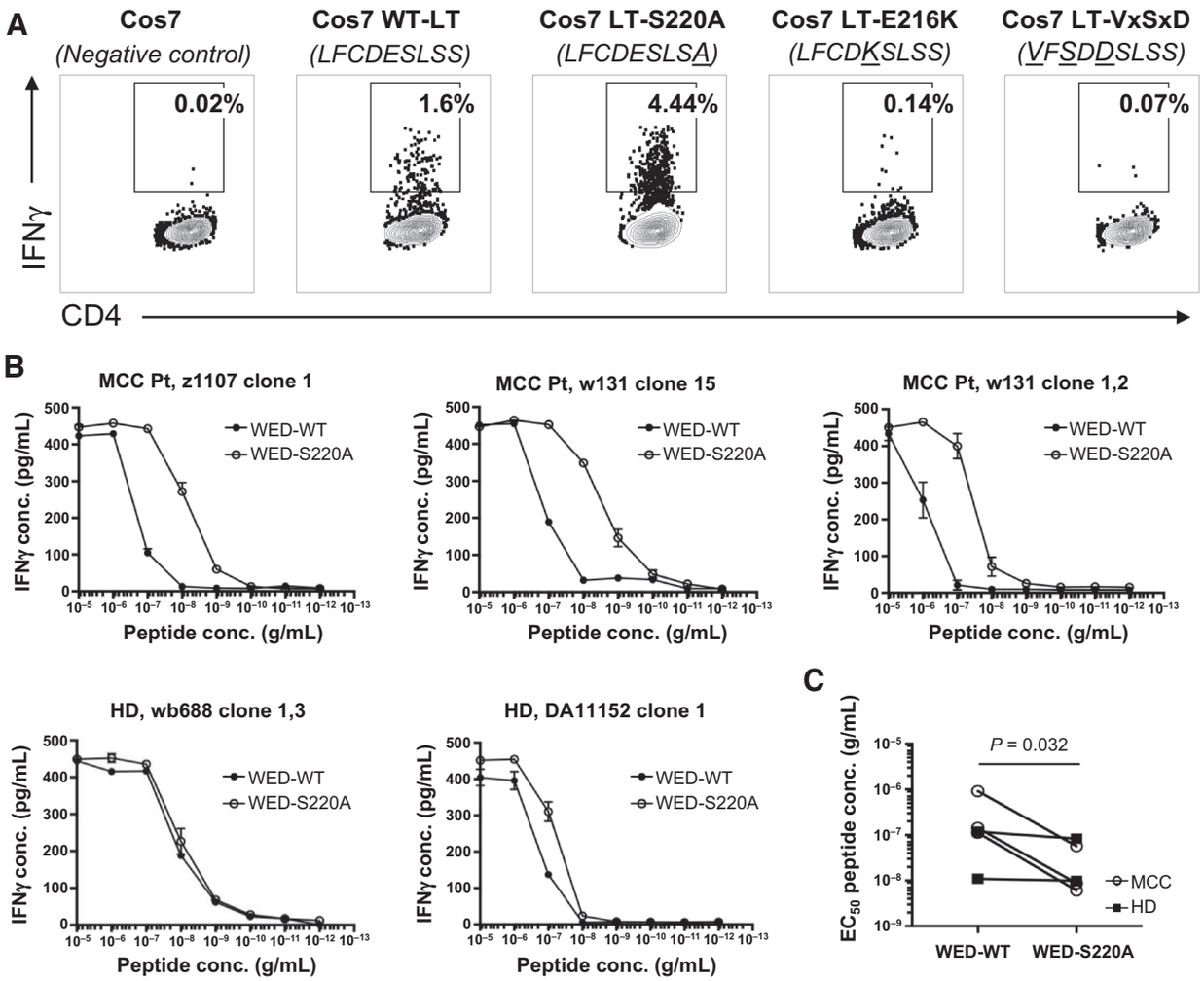

Figure 6.

$WED_{LT209\text{-}228}$–specific $CD4^+$ T-cell clones can recognize mutant S220A but not E216K. **A,** A $WED_{LT209\text{-}228}$–specific clone (wb688 clone 1,3) was incubated with DRB1*0401-positive PBMCs (as APCs) and COS-7 cell lysates that were either untransfected (negative control), transfected with wild-type (WT) LT, or mutant LT-S220A, LT-E216K, or LT-VxSxD. Intracellular IFNγ was measured by ICS. Flow plots are representative data of four HLA-DRB1*0401–restricted clones. The percentage of viable $CD4^+IFN\gamma^+$ T cells (CFSE-labeled APCs excluded and negative for CD8/CD14/CD19) in the lymphocyte forward/side scatter region is denoted. **B,** Dose–response curves of a $WED_{LT209\text{-}228}$–specific HLA-DRB1*0401–restricted CD4 clones stimulated with $WED_{LT209\text{-}228}$ (WED-WT) or $WED_{LT209\text{-}228}$-S220A peptides. Clones were incubated with HLA-DRB1*0401–positive LCLs (as APCs) and peptides. IFNγ secretion was measured by ELISA. Of the five clones tested, three were from MCC patients (MCC) and two were from healthy donors (HD). Lines connect means. Error bars denote standard deviation. **C,** Dose–response curves were used to calculate the EC_{50} of five distinct $WED_{LT209\text{-}228}$–specific HLA-DRB1*0401–restricted $CD4^+$ T-cell clones for WED-WT or WED-S220A peptides. Wilcoxon matched-pairs signed rank test was used to compare EC_{50} values. *P* value is shown.

harnessing tumor-specific $CD4^+$ T cells can improve immune-based therapies and sustain $CD8^+$ T-cell responses (44). Specifically, infusion of autologous TILs, which contain both $CD4^+$ and $CD8^+$ T cells, has shown higher response rates (50%–70%) in malignant melanoma than have $CD8^+$ T cells alone (45). A study has described the case of a stage IV acral melanoma patient who experienced a complete response after TIL therapy, which included $CD4^+$ T cells specific for BRAF-V600E. These tumor-specific $CD4^+$ T cells increased in frequency within the blood after therapy and persisted long term, suggesting that these cells were of clinical significance and augmented the antitumor immune response (46). Administration of autologous cancer-specific $CD4^+$ T cells has mediated regression of distant metastatic disease in epithelial cholangiocarcinoma (17) and complete clinical remission in another patient with metastatic melanoma (16). The use of genetically engineered $CD4^+$ T cells targeting melanoma-associated antigen-A3 (MAGE-A3) yields objective responses among patients with esophageal cancer, urothelial cancer, and osteosarcoma (18), indicating that cellular therapy utilizing $CD4^+$ T cells has powerful therapeutic potential in a wide array of solid cancers. Clinical trials utilizing neoantigen-based therapeutic vaccines for melanoma have yielded impressive clinical responses that correlate with robust $CD4^+$ T-cell stimulation, particularly in the setting of combined PD-1 blockade therapy (20, 21). Against this backdrop, our identification of $CD4^+$ T-cell epitopes and the generation of four HLA

Published OnlineFirst August 12, 2019; DOI: 10.1158/2326-6066.CIR-19-0103

class II multimers (tetramers/dextramers) facilitated the characterization of MCPyV-specific CD4$^+$ T-cell responses and the subsequent development of CD4-targeted therapies for MCC, including a therapeutic cancer vaccine.

Vaccination approaches targeting MCPyV oncoproteins have clinical appeal for several reasons. Viral antigens are shared among MCC patients and, therefore, could be used to generate "off-the-shelf" vaccines that are not patient specific. Indeed, MCPyV LT and sT are immunogenic, containing at least 35 known T-cell epitopes (28 CD8 and 7 CD4), including WED$_{LT209\text{-}228}$, and are restricted by diverse HLA class I and II alleles, suggesting that an MCPyV oncoprotein vaccine has the potential to induce T-cell immunity in most MCC patients (24, 47–50). To date, two groups have described potential MCPyV therapeutic vaccine strategies utilizing both *in vivo* (50) and *ex vivo* models (51). Both studies indicate the ability to induce MCPyV-specific immunity following vaccination with the MCPyV LT antigen. However, additional work is required to translate these findings to the clinic.

Importantly, vaccination with MCPyV T-antigens in humans raises safety concerns due to the known oncogenic activity of these proteins. Approaches to "detoxify" oncogene-based cancer vaccines have shown promising safety profiles and efficacy in treating HPV-induced premalignant lesions (52). These "detoxified" vaccines harbored mutations within the LxCxE motif of the HPV-E7 oncoprotein, suggesting that a similar approach in the context of MCPyV LT may be possible (52). One possible "detoxification" strategy would be to simply delete the LxCxE region. However, this would result in loss of the immunogenic WED$_{LT209\text{-}228}$ CD4 epitope. Notably, two point mutations within the LxCxE region at residue 216 (E216K mutation) or 220 (S220A mutation) have been reported to prevent Rb binding, thereby blocking oncogenic activity at this site (4, 5, 40). However, we showed that of these two mutations, only S220A retained the relevant epitope that allowed recognition by HLA-DRB1*0401–restricted WED$_{LT209\text{-}228}$–specific T-cell clones. Collectively, these data indicated that the WED$_{LT209\text{-}228}$ epitope is immunogenic, expressed within MCC tumors, and could be "detoxified" through mutating S220 without disrupting antigenicity.

There are several limitations of our studies. First, it is unlikely that we identified all relevant CD4 epitopes within the MCPyV oncoproteins. Study of additional MCC patients, as well as other methods of epitope identification, may yield additional disease-relevant epitopes (53). The peptide lengths used in our initial mapping studies were 13-mers, but minimal CD4$^+$ T-cell epitopes can sometimes be longer, and indeed, other groups have reported using different lengths or RNA-transfected APCs encoding the antigen of interest for CD4 epitope mapping studies (54). Consequently, alternative antigen formats could be utilized to more comprehensively map CD4 epitopes within the MCPyV T-antigens. The characterization of WED$_{LT209\text{-}228}$ reported here was largely carried forward in the context of the HLA-DRB1*0401 allele. Therefore, additional research is required to fully characterize the response to WED$_{LT209\text{-}228}$ in the context of HLA-DRB1*0301 and HLA-DQB1*0301.

The findings reported here have key implications for future investigation and clinical applications. The ability to deeply probe the immunobiology of this disease using the tools described herein provides a powerful opportunity to understand tumor-specific T-cell responses against a shared tumor antigen. Although checkpoint inhibitors have revolutionized cancer therapy, only half of MCC patients experience durable responses (10–12). Therefore, the development of novel therapies including cancer vaccines and/or CD4$^+$ T-cell therapy may provide much-needed adjunctive therapeutic strategies for MCC patients and cancer patients.

Disclosure of Potential Conflicts of Interest

K.G. Paulson reports receiving other commercial research support from Merck-SITC. P. Nghiem is a consultant/advisory board member for EMD Serono and Merck. D.M. Koelle reports receiving a commercial research grant from Immunomics Therapeutics. No potential conflicts of interest were disclosed by the other authors.

Authors' Contributions

Conception and design: N.V. Longino, P. Nghiem, W.W. Kwok, D.M. Koelle
Development of methodology: N.V. Longino, J. Yang, E.A. James, P. Nghiem, W.W. Kwok, D.M. Koelle
Acquisition of data (provided animals, acquired and managed patients, provided facilities, etc.): N.V. Longino, J. Yang, J.G. Iyer, D. Ibrani, K.J. Laing, V.L. Campbell, K.G. Paulson, R.M. Kulikauskas, C.D. Church, P. Nghiem
Analysis and interpretation of data (e.g., statistical analysis, biostatistics, computational analysis): N.V. Longino, J. Yang, K.J. Laing, C.D. Church, W.W. Kwok, D.M. Koelle
Writing, review, and/or revision of the manuscript: N.V. Longino, J.G. Iyer, I.-T. Chow, K.J. Laing, V.L. Campbell, K.G. Paulson, C.D. Church, E.A. James, P. Nghiem, W.W. Kwok, D.M. Koelle
Administrative, technical, or material support (i.e., reporting or organizing data, constructing databases): N.V. Longino, D. Ibrani, I.-T. Chow, K.J. Laing, P. Nghiem
Study supervision: N.V. Longino, P. Nghiem, W.W. Kwok

Acknowledgments

The authors would like to thank David Crispin and Martin McIntosh for their assistance in the sequencing of CD4$^+$ T-cell receptors. This study was supported by grants 1P01CA225517, 5K24CA139052-10, NIH T32ES007032, and P30-CA01570.

The costs of publication of this article were defrayed in part by the payment of page charges. This article must therefore be hereby marked *advertisement* in accordance with 18 U.S.C. Section 1734 solely to indicate this fact.

Received February 10, 2019; revised May 7, 2019; accepted August 6, 2019; published first August 12, 2019.

References

1. Lemos BD, Storer BE, Iyer JG, Phillips JL, Bichakjian CK, Fang LC, et al. Pathologic nodal evaluation improves prognostic accuracy in Merkel cell carcinoma: analysis of 5823 cases as the basis of the first consensus staging system. J Am Acad Dermatol 2010;63:751–61.
2. Paulson KG, Park SY, Vandeven NA, Lachance K, Thomas H, Chapuis AG, et al. Merkel cell carcinoma: current US incidence and projected increases based on changing demographics. J Am Acad Dermatol 2018;78:457–63.e2.
3. Feng H, Shuda M, Chang Y, Moore PS. Clonal integration of a polyomavirus in human Merkel cell carcinoma. Science 2008;319:1096–100.
4. Shuda M, Feng H, Kwun HJ, Rosen ST, Gjoerup O, Moore PS, et al. T antigen mutations are a human tumor-specific signature for Merkel cell polyomavirus. PNAS 2008;105:16272–7.
5. Houben R, Adam C, Baeurle A, Hesbacher S, Grimm J, Angermeyer S, et al. An intact retinoblastoma protein-binding site in Merkel cell polyomavirus

large T antigen is required for promoting growth of Merkel cell carcinoma cells. Int J Cancer 2012;130:847–56.
6. Sobhy H. A review of functional motifs utilized by viruses. Proteomes 2016;4. pii:E3.
7. Lau L, Gray EE, Brunette RL, Stetson DB. DNA tumor virus oncogenes antagonize the cGAS-STING DNA-sensing pathway. Science 2015;350: 568–71.
8. Houben R, Shuda M, Weinkam R, Schrama D, Feng H, Chang Y, et al. Merkel cell polyomavirus-infected Merkel cell carcinoma cells require expression of viral T antigens. J Virol 2010;84:7064–72.
9. Shuda M, Chang Y, Moore PS. Merkel cell polyomavirus-positive Merkel cell carcinoma requires viral small T-antigen for cell proliferation. J Invest Dermatol 2014;134:1479–81.
10. Nghiem PT, Bhatia S, Lipson EJ, Kudchadkar RR, Miller NJ, Annamalai L, et al. PD-1 blockade with pembrolizumab in advanced merkel-cell carcinoma. N Engl J Med 2016;374:2542–52.
11. D'Angelo SP, Russell J, Lebbe C, Chmielowski B, Gambichler T, Grob JJ, et al. Efficacy and safety of first-line avelumab treatment in patients with stage IV metastatic merkel cell carcinoma: a preplanned interim analysis of a clinical trial. JAMA Oncol 2018;4:e180077.
12. Topalian SL, Bhatia S, Hollebecque A, Awada A, De Boer JP, Kudchadkar RR, et al. Non-comparative, open-label, multiple cohort, phase 1/2 study to evaluate nivolumab (NIVO) in patients with virus-associated tumors (CheckMate 358): efficacy and safety in Merkel cell carcinoma (MCC) [abstract]. In: Proceedings of the American Association for Cancer Research Annual Meeting 2017; 2017 Apr 1–5; Washington, DC. Philadelphia (PA): AACR; Cancer Res 2017;77(13 Suppl):Abstract nr CT074. doi: 10.1158/1538-7445.AM2017-CT074.
13. Paulson KG, Iyer JG, Tegeder AR, Thibodeau R, Schelter J, Koba S, et al. Transcriptome-wide studies of merkel cell carcinoma and validation of intratumoral CD8+ lymphocyte invasion as an independent predictor of survival. J Clin Oncol 2011;29:1539–46.
14. Paulson KG, Iyer JG, Simonson WT, Blom A, Thibodeau RM, Schmidt M, et al. CD8+ lymphocyte intratumoral infiltration as a stage-independent predictor of Merkel cell carcinoma survival: a population-based study. Am J Clin Pathol 2014;142:452–8.
15. Turtle CJ, Hanafi LA, Berger C, Gooley TA, Cherian S, Hudecek M, et al. CD19 CAR-T cells of defined CD4+:CD8+ composition in adult B cell ALL patients. J Clin Invest 2016;126:2123–38.
16. Hunder NN, Wallen H, Cao J, Hendricks DW, Reilly JZ, Rodmyre R, et al. Treatment of metastatic melanoma with autologous CD4+ T cells against NY-ESO-1. N Engl J Med 2008;358:2698–703.
17. Tran E, Turcotte S, Gros A, Robbins PF, Lu YC, Dudley ME, et al. Cancer immunotherapy based on mutation-specific CD4+ T cells in a patient with epithelial cancer. Science 2014;344:641–5.
18. Lu YC, Parker LL, Lu T, Zheng Z, Toomey MA, White DE, et al. Treatment of patients with metastatic cancer using a major histocompatibility complex class II-Restricted T-cell receptor targeting the cancer germline antigen MAGE-A3. J Clin Oncol 2017;35:3322–9.
19. Kreiter S, Vormehr M, van de Roemer N, Diken M, Lower M, Diekmann J, et al. Mutant MHC class II epitopes drive therapeutic immune responses to cancer. Nature 2015;520:692–6.
20. Ott PA, Hu Z, Keskin DB, Shukla SA, Sun J, Bozym DJ, et al. An immunogenic personal neoantigen vaccine for patients with melanoma. Nature 2017;547:217–21.
21. Sahin U, Derhovanessian E, Miller M, Kloke BP, Simon P, Lower M, et al. Personalized RNA mutanome vaccines mobilize poly-specific therapeutic immunity against cancer. Nature 2017;547:222–6.
22. Zhao LP, Carlsson A, Larsson HE, Forsander G, Ivarsson SA, Kockum I, et al. Building and validating a prediction model for paediatric type 1 diabetes risk using next generation targeted sequencing of class II HLA genes. Diabetes Metab Res Rev 2017;33. doi: 10.1002/dmrr.2921.
23. Gersuk VH, Nepom GT.A real-time polymerase chain reaction assay for the rapid identification of the autoimmune disease-associated allele HLA-DQB1*0602. Tissue Antigens 2009;73:335–40.
24. Iyer JG, Afanasiev OK, McClurkan C, Paulson K, Nagase K, Jing L, et al. Merkel cell polyomavirus-specific CD8(+) and CD4(+) T-cell responses identified in Merkel cell carcinomas and blood. Clin Cancer Res 2011;17: 6671–80.
25. Afanasiev OK, Yelistratova L, Miller N, Nagase K, Paulson K, Iyer JG, et al. Merkel polyomavirus-specific T cells fluctuate with merkel cell carcinoma burden and express therapeutically targetable PD-1 and Tim-3 exhaustion markers. Clin Cancer Res 2013;19:5351–60.
26. Rosen ST, Gould VE, Salwen HR, Herst CV, Le Beau MM, Lee I, et al. Establishment and characterization of a neuroendocrine skin carcinoma cell line. Lab Invest 1987;56:302–12.
27. Leonard JH, Dash P, Holland P, Kearsley JH, Bell JR. Characterisation of four Merkel cell carcinoma adherent cell lines. Int J Cancer 1995;60: 100–7.
28. Novak EJ, Liu AW, Gebe JA, Falk BA, Nepom GT, Koelle DM, et al. Tetramer-guided epitope mapping: rapid identification and characterization of immunodominant CD4+ T cell epitopes from complex antigens. J Immunol 2001;166:6665–70.
29. Cai G, Hafler DA.Multispecific responses by T cells expanded by endogenous self-peptide/MHC complexes. Eur J Immunol 2007;37:602–12.
30. Pawelec G, Fernandez N, Brocker T, Schneider EM, Festenstein H, Wernet P. DY determinants, possibly associated with novel class II molecules, stimulate autoreactive CD4+ T cells with suppressive activity. J Exp Med 1988; 167:243–61.
31. Koelle DM, Corey L, Burke RL, Eisenberg RJ, Cohen GH, Pichyangkura R, et al. Antigenic specificities of human CD4+ T-cell clones recovered from recurrent genital herpes simplex virus type 2 lesions. J Virol 1994;68: 2803–10.
32. Koelle DM, Abbo H, Peck A, Ziegweid K, Corey L. Direct recovery of herpes simplex virus (HSV)-specific T lymphocyte clones from recurrent genital HSV-2 lesions. J Infect Dis 1994;169:956–61.
33. Miller NJ, Church CD, Dong L, Crispin D, Fitzgibbon MP, Lachance K, et al. Tumor-infiltrating merkel cell polyomavirus-specific T cells are diverse and associated with improved patient survival. Cancer Immunol Res 2017;5: 137–47.
34. Sihto H, Bohling T, Kavola H, Koljonen V, Salmi M, Jalkanen S, et al. Tumor infiltrating immune cells and outcome of Merkel cell carcinoma: a population-based study. Clin Cancer Res 2012;18:2872–81.
35. Neller MA, Lai MH, Lanagan CM, O'Connor LE, Pritchard AL, Martinez NR, et al. High efficiency ex vivo cloning of antigen-specific human effector T cells. PLoS One 2014;9:e110741.
36. Massilamany C, Gangaplara A, Jia T, Elowsky C, Kang G, Riethoven JJ, et al. Direct staining with major histocompatibility complex class II dextramers permits detection of antigen-specific, autoreactive CD4 T cells in situ. PLoS One 2014;9:e87519.
37. Becker C, Pohla H, Frankenberger B, Schuler T, Assenmacher M, Schendel DJ, et al. Adoptive tumor therapy with T lymphocytes enriched through an IFN-gamma capture assay. Nat Med 2001;7:1159–62.
38. Oyarzun P, Ellis JJ, Boden M, Kobe B. PREDIVAC: CD4+ T-cell epitope prediction for vaccine design that covers 95% of HLA class II DR protein diversity. BMC Bioinformatics 2013;14:52.
39. Holland CJ, Cole DK, Godkin A. Re-Directing CD4(+) T cell responses with the flanking residues of MHC class II-bound peptides: the core is not enough. Front Immunol 2013;4:172.
40. Schrama D, Hesbacher S, Angermeyer S, Schlosser A, Haferkamp S, Aue A, et al. Serine 220 phosphorylation of the Merkel cell polyomavirus large T antigen crucially supports growth of Merkel cell carcinoma cells. Int J Cancer 2015;138:1153–62.
41. Su LF, Kidd BA, Han A, Kotzin JJ, Davis MM. Virus-specific CD4(+) memory-phenotype T cells are abundant in unexposed adults. Immunity 2013;38:373–83.
42. Kim HJ, Cantor H. CD4 T-cell subsets and tumor immunity: the helpful and the not-so-helpful. Cancer Immunol Res 2014;2:91–8.
43. Bacher P, Scheffold A.Flow-cytometric analysis of rare antigen-specific T cells. Cytometry A 2013;83:692–701.
44. Muranski P, Restifo NP.Adoptive immunotherapy of cancer using CD4(+) T cells. Curr Opin Immunol 2009;21:200–8.
45. Dudley ME, Yang JC, Sherry R, Hughes MS, Royal R, Kammula U, et al. Adoptive cell therapy for patients with metastatic melanoma: evaluation of intensive myeloablative chemoradiation preparative regimens. J Clin Oncol 2008;26:5233–9.
46. Veatch JR, Lee SM, Fitzgibbon M, Chow IT, Jesernig B, Schmitt T, et al. Tumor-infiltrating BRAFV600E-specific CD4+ T cells correlated with complete clinical response in melanoma. J Clin Invest 2018;128: 1563–8.
47. Chapuis AG, Afanasiev OK, Iyer JG, Paulson KG, Parvathaneni U, Hwang JH, et al. Regression of metastatic Merkel cell carcinoma following transfer

Published OnlineFirst August 12, 2019; DOI: 10.1158/2326-6066.CIR-19-0103

of polyomavirus-specific T cells and therapies capable of re-inducing HLA class-I. Cancer Immunol Res 2014;2:27–36.
48. Lyngaa R, Pedersen NW, Schrama D, Thrue CA, Ibrani D, Met O, et al. T-cell responses to oncogenic merkel cell polyomavirus proteins distinguish patients with merkel cell carcinoma from healthy donors. Clin Cancer Res 2014;20:1768–78.
49. Ibrani D, Iyer J, Miller N, Vandeven N, Afanasiev O, Koelle D, et al. Identifying Merkel polyomavirus-specific CD4+ and CD8+ T-cells in Merkel cell carcinoma patients' tumor-infiltrating lymphocytes. Presented at the 2015 Society for Investigative Dermatology Annual Meeting; 2015 May 6–9; Atlanta, GA. Cleveland (OH): SID; 2015.
50. Zeng Q, Gomez BP, Viscidi RP, Peng S, He L, Ma B, et al. Development of a DNA vaccine targeting Merkel cell polyomavirus. Vaccine 2012;30:1322–9.
51. Gerer KF, Erdmann M, Hadrup SR, Lyngaa R, Martin LM, Voll RE, et al. Preclinical evaluation of NF-kappaB-triggered dendritic cells expressing the viral oncogenic driver of Merkel cell carcinoma for therapeutic vaccination. Ther Adv Med Oncol 2017;9:451–64.
52. Alvarez RD, Huh WK, Bae S, Lamb LS Jr., Conner MG, Boyer J, et al. A pilot study of pNGVL4a-CRT/E7(detox) for the treatment of patients with HPV16+ cervical intraepithelial neoplasia 2/3 (CIN2/3). Gynecol Oncol 2016;140:245–52.
53. Provenzano M, Panelli MC, Mocellin S, Bracci L, Sais G, Stroncek DF, et al. MHC-peptide specificity and T-cell epitope mapping: where immunotherapy starts. Trends Mol Med 2006;12:465–72.
54. Simon P, Omokoko TA, Breitkreuz A, Hebich L, Kreiter S, Attig S, et al. Functional TCR retrieval from single antigen-specific human T cells reveals multiple novel epitopes. Cancer Immunol Res 2014;2:1230–44.

Published OnlineFirst August 12, 2019; DOI: 10.1158/2326-6066.CIR-19-0103

Cancer Immunology Research

Human CD4$^+$ T Cells Specific for Merkel Cell Polyomavirus Localize to Merkel Cell Carcinomas and Target a Required Oncogenic Domain

Natalie V. Longino, Junbao Yang, Jayasri G. Iyer, et al.

Cancer Immunol Res 2019;7:1727-1739. Published OnlineFirst August 12, 2019.